

# Exploring Cyclic Expansion and Contraction in Brans-Dicke Theory through Periodic Deceleration

Rahul Sharma, R.K. Mishra 

Department of Mathematics, Sant Longowal Institute of Engineering and Technology, Longowal-148106, Punjab, India

Received 25 October 2025

**Abstract.** In this study, we investigate the cyclic evolution of the Universe within the framework of Brans–Dicke theory (BDT) by adopting a periodic varying deceleration parameter (PVDP). The proposed model consistently captures the complete cosmic cycle—birth, expansion, slow-down, contraction, and rebirth—thus realizing a bouncing or oscillatory cosmology. The dynamical behavior of fundamental kinematic quantities, including the Hubble parameter, scale factor, and directional expansion rates, substantiates this recurrent evolution. Furthermore, cosmological parameters derived from the modified field equations—such as energy density, pressure, the cosmological constant, and the equation of state (EoS) parameter—exhibit patterns that align with the cyclic nature of the Universe. To strengthen this analysis, higher-order cosmographic parameters (jerk, snap, and lerk) are also computed and examined with respect to cosmic time, providing refined insights into the model’s dynamical consistency. The interplay between these parameters reinforces the oscillatory features of the Universe and demonstrates agreement with observationally motivated phases of cosmic evolution. Overall, our findings highlight that Brans–Dicke theory, supplemented by a PVDP, offers a compelling framework for exploring cyclic cosmology beyond the standard  $\Lambda$ CDM paradigm.

**KEY WORDS:** Accelerating universe, Brans-Dicke theory, cosmological models, deceleration parameter.

## 1 Introduction

Recent astronomical observations, including type-Ia supernovae, baryon acoustic oscillations, and cosmic microwave background (CMB) measurements, confirm that we are living in an expanding and accelerating Universe [1–5]. This accelerated expansion is attributed to an exotic component known as dark energy (DE), characterized by negative pressure, which drives the rapid growth

of the cosmic scale. While the standard  $\Lambda$ CDM model has provided an excellent concordance framework for explaining these phenomena, it relies on the assumption of a constant deceleration parameter (DP) [6]. However, recent investigations suggest that the expansion history of the Universe may involve more complex dynamics, with possible transitions between decelerating and accelerating phases. Such deviations from  $\Lambda$ CDM have motivated the exploration of alternative cosmological models and modified theories of gravity [7–18].

Among these, Brans–Dicke theory (BDT) has received significant attention due to its incorporation of a dynamical scalar field that couples with the metric, introducing a time-dependent gravitational constant [19]. The theory, governed by the Brans–Dicke coupling parameter ( $\omega$ ), offers a flexible framework to examine the Universe beyond general relativity and provides new pathways to explain cosmic evolution. Several researchers have developed cosmological models within BDT by adopting different functional forms of the DP, leading to diverse insights into the Universe’s dynamical history [20–26].

In this work, we investigate the dynamics of the Universe in the framework of BDT under the assumption of a periodic varying deceleration parameter (PVDP) [27]. This choice is motivated by its ability to describe alternating epochs of acceleration and deceleration, thereby capturing the possibility of cyclic or bouncing cosmological behavior [28–32]. Such a scenario naturally accounts for repeated phases of expansion, contraction, and rebirth of the Universe, which may shed light on its large-scale structure and long-term fate. By employing both analytical and numerical techniques, we analyze the consequences of this periodically varying DP on kinematic quantities, energy density, pressure, cosmological constant, and the equation of state (EoS) parameter derived from the modified field equations.

Furthermore, we extend our analysis to higher-order cosmographic parameters such as jerk, snap, and lerk, which offer refined diagnostics of cosmic evolution. The evolution of these parameters with cosmic time provides deeper insight into the oscillatory nature of the model and strengthens the interpretation of the Universe as cyclic within the BDT framework. This investigation not only contributes to our understanding of the role of DE and scalar–tensor gravity but also highlights the potential of periodic cosmic dynamics to address fundamental questions about the origin, evolution, and possible recurrence of the Universe.

This study is organized into six sections. In Section 2, we present the metric and the basic field equations of the model. Section 3 outlines the assumptions adopted for constructing the model. In Section 4, we solve the field equations and discuss the fundamental properties of the model. The energy conditions are examined separately in Section 4.1. Section 5 is devoted to higher-order analyses, where cosmographic parameters are explored in Section 5.1, followed by the statefinder diagnostic in Section 5.2. Finally, Section 6 provides the concluding remarks of the study.

## 2 Metric and Brans-Dicke Equations Describe Different Gravitational Interactions

In order to study the anisotropic nature of the early Universe, we consider the Bianchi type-I (BI) spacetime, which is the simplest among the Bianchi class of homogeneous cosmological models. Unlike the isotropic Friedmann-Lemaître–Robertson–Walker (FLRW) metric, the BI spacetime allows for anisotropic expansion along three mutually orthogonal spatial directions while maintaining spatial homogeneity. This feature makes it an appropriate framework to investigate the influence of anisotropy on cosmic dynamics, particularly in the early Universe when anisotropic effects are believed to be significant. Moreover, as the Universe evolves, the BI model naturally approaches isotropy, making it consistent with the observed large-scale structure of the present Universe.

Accordingly, the line element of the homogeneous and anisotropic BI spacetime is taken as

$$ds^2 = dt^2 - R_1^2(t)dx^2 - R_2^2(t)dy^2 - R_3^2(t)dz^2, \quad (1)$$

where  $R_1(t)$ ,  $R_2(t)$ , and  $R_3(t)$  represent the directional scale factors along the  $x$ ,  $y$ , and  $z$  axes, respectively. The energy-momentum tensor (EMT)  $T_{kl}$  for a perfect cosmic fluid is described as follows

$$T_{kl} = (\rho + p)u_k u_l - g_{kl}p. \quad (2)$$

In this context,  $\rho$  represents the energy density,  $p$  stands for isotropic pressure, and  $u_k = (1, 0, 0, 0)$  denotes the four-velocity vector, obeying the condition  $g_{kl}u^k u^l = 1$ . As mentioned in the introduction, in this communication, we formulate a cosmological model within the framework of BDT. The field equations in this theory are defined as follows:

$$R_{kl} - \frac{1}{2}g_{kl}R = \frac{8\pi}{\phi}T_{kl} + \frac{\omega}{\phi^2}(\phi_{,k}\phi_{,l} - \frac{1}{2}g_{kl}\phi_{,\alpha}\phi^{,\alpha}) + \frac{1}{\phi}(\phi_{;k;l} - g_{kl}\square\phi) - \Lambda g_{kl}, \quad (3)$$

$$\square\phi = \frac{1}{2\omega + 3}(8\pi T + 2\Lambda\phi), \quad (4)$$

where  $R_{kl}$  stands for the Ricci tensor,  $g_{kl}$  represents the metric tensor,  $R$  is the Ricci scalar,  $\phi$  is the scalar field,  $\omega$  is a dimensionless coupling constant, and  $\phi_{,k}$  (or simply  $\phi_k$ ) represents the ordinary derivative of  $\phi$  with respect to  $x^k$ , and  $\square$  is the d'Alembertian operator,  $\nabla$  is a Laplacian operator,  $\Lambda$  is a cosmological constant and  $T = T_k^k$  is the trace of EMT  $T_{kl}$ .

For BI space time, the field equations (3) takes the form

$$\frac{\dot{R}_3\dot{R}_1}{R_3R_1} + \frac{\dot{R}_1\dot{R}_2}{R_1R_2} + \frac{\dot{R}_2\dot{R}_3}{R_2R_3} - \frac{\omega}{2}\left(\frac{\dot{\phi}}{\phi}\right)^2 + \frac{\dot{\phi}}{\phi}\left(\frac{\dot{R}_1}{R_1} + \frac{\dot{R}_2}{R_2} + \frac{\dot{R}_3}{R_3}\right) = \frac{8\pi\rho}{\phi} + \Lambda, \quad (5)$$

#### 4 Exploring Cyclic Expansion and Contraction in Brans-Dicke Theory ...

$$\frac{\ddot{R}_2}{R_2} + \frac{\ddot{R}_3}{R_3} + \frac{\dot{R}_2\dot{R}_3}{R_2R_3} + \frac{\omega}{2} \left(\frac{\dot{\phi}}{\phi}\right)^2 + \frac{\dot{\phi}}{\phi} \left(\frac{\dot{R}_2}{R_2} + \frac{\dot{R}_3}{R_3}\right) + \frac{\ddot{\phi}}{\phi} = -\frac{8\pi p}{\phi} + \Lambda, \quad (6)$$

$$\frac{\ddot{R}_1}{R_1} + \frac{\ddot{R}_3}{R_3} + \frac{\dot{R}_3\dot{R}_1}{R_3R_1} + \frac{\omega}{2} \left(\frac{\dot{\phi}}{\phi}\right)^2 + \frac{\dot{\phi}}{\phi} \left(\frac{\dot{R}_1}{R_1} + \frac{\dot{R}_3}{R_3}\right) + \frac{\ddot{\phi}}{\phi} = -\frac{8\pi p}{\phi} + \Lambda, \quad (7)$$

$$\frac{\ddot{R}_1}{R_1} + \frac{\ddot{R}_2}{R_2} + \frac{\dot{R}_2\dot{R}_1}{R_2R_1} + \frac{\omega}{2} \left(\frac{\dot{\phi}}{\phi}\right)^2 + \frac{\dot{\phi}}{\phi} \left(\frac{\dot{R}_1}{R_1} + \frac{\dot{R}_2}{R_2}\right) + \frac{\ddot{\phi}}{\phi} = -\frac{8\pi p}{\phi} + \Lambda, \quad (8)$$

$$\frac{\ddot{\phi}}{\phi} + \frac{\dot{\phi}}{\phi} \left(\frac{\dot{R}_1}{R_1} + \frac{\dot{R}_2}{R_2} + \frac{\dot{R}_3}{R_3}\right) = -\frac{8\pi(3p - \rho)}{(2\omega + 3)\phi} + \frac{2\Lambda}{2\omega + 3}. \quad (9)$$

Before proceeding to the solutions of the field equations, it is essential to introduce a set of fundamental physical parameters that characterize the dynamical properties of the Universe. These parameters play a pivotal role in quantifying the processes of expansion, contraction, and overall evolution of the cosmos on large scales. Within the framework of cosmological theories, they not only provide valuable insights into the global structure of the Universe but also serve as diagnostic tools for interpreting its past, present, and future behavior.

One such key quantity is the average scale factor  $a(t)$ , which represents the effective measure of cosmic expansion when anisotropy is present. Constructed from the directional scale factors along the three spatial axes, it is defined through their geometric mean. This formulation encapsulates the overall deformation of the spacetime fabric and offers a unified description of the cosmic size. The value of  $a(t)$  acts as a direct indicator of the dynamical state of the Universe—growth ( $a(t) > 1$ ) corresponds to expansion, shrinkage ( $a(t) < 1$ ) to contraction, while constancy ( $a(t) = 1$ ) denotes equilibrium or stasis.

$$a(t) = \sqrt[3]{R_1(t)R_2(t)R_3(t)}. \quad (10)$$

The generalized mean Hubble parameter  $H$  is obtained by taking the arithmetic average of three individual Hubble parameters and is defined as

$$H = \frac{1}{3}(H_1 + H_2 + H_3), \quad (11)$$

this parameter provides a way to characterize the overall rate of cosmic expansion based on these individual Hubble parameters.

Spatial volume ( $V$ ) represents the 3D-extent of the universe at a given cosmic moment, reflecting both its size and geometric properties. It is determined by the scale factor  $a(t)$  and provides insights into the universe's evolving dimensions and structure which helps to study the dynamic expansion or contraction.

$$V(t) = R_1(t)R_2(t)R_3(t). \quad (12)$$

Expansion scalar ( $\theta$ ) in cosmology measures the rate at which the volume of the universe changes with time. It is a crucial parameter in understanding cosmic expansion dynamics

$$\theta = 3H = \frac{\dot{R}_1}{R_1} + \frac{\dot{R}_2}{R_2} + \frac{\dot{R}_3}{R_3}. \quad (13)$$

Shear Scalar ( $\sigma$ ), characterizes the anisotropy or stretching of spatial dimensions within the universe. It measures how space deforms as the universe expands and is a key element in studying cosmic structure formation and is defined as

$$\sigma^2 = \frac{1}{2} \sum_{i=1}^3 H_i^2 - \frac{1}{6} \theta^2, \quad i = 1, 2, 3. \quad (14)$$

Mean anisotropic parameter ( $A_m$ ), quantifies the degree of anisotropy in the universe. It provides insights into the homogeneity and isotropy of the cosmos. In Bianchi cosmologies,  $A_m$  is used to characterize the anisotropic expansion and is defined as

$$A_m = \frac{1}{3} \sum_{i=1}^3 \left( \frac{\Delta H_i}{H} \right)^2. \quad (15)$$

Deceleration parameter ( $q(t)$ ) characterizes whether the cosmic expansion is accelerating or decelerating. A positive  $q$  indicates a decelerating universe, where gravitational forces slow down the expansion. Conversely, a negative  $q$  signifies cosmic acceleration, where dark energy's influence drives an increasingly rapid expansion and is defined as

$$q(t) = -\frac{\ddot{a}a}{\dot{a}^2}. \quad (16)$$

In the next section, we have obtained the solutions for the field equations and calculated the values of the required parameters by taking suitable viable assumptions.

### 3 Assumptions of the model

The system of field equations (5)–(9) contains more unknowns than the number of available independent equations. To obtain explicit solutions, it is therefore necessary to impose additional constraints among the variables. In the present work, we adopt two such constraints: a PVDP, originally proposed by Shen and Zhao [27] and given in equation (17), along with a power-law relation between the scale factor  $a$  and the scalar field  $\phi$ , as proposed by Johri and Desikan (1994) [33] and expressed in equation (22). These choices not only reduce the level of indeterminacy but also provide a natural framework for exploring oscillatory cosmic dynamics. In particular, the PVDP enables the Universe to experience

## 6 Exploring Cyclic Expansion and Contraction in Brans-Dicke Theory ...

successive epochs of acceleration and deceleration, thereby supporting the study of its cyclic or bouncing nature within the Brans–Dicke framework.

$$q(t) = -1 + \frac{k \cot(kt)}{H}, \quad (17)$$

where  $k$  is positive constant. Now by solving equation (17) with the help of equation (16) we find the value of Hubble parameter  $H$  and the scale factor  $a(t)$  and are written as

$$H(t) = \frac{1}{\alpha \sin(kt)}, \quad (18)$$

$$a(t) = \left[ n \tan\left(\frac{kt}{2}\right) \right]^{\frac{1}{\alpha}}, \quad (19)$$

where  $n$  is the constant of integration and we take  $n = 1$  therefore above equation becomes

$$a(t) = \left[ \tan\left(\frac{kt}{2}\right) \right]^{\frac{1}{\alpha}}. \quad (20)$$

After substituting the Hubble parameter into equation (17), we obtain the DP as

$$q(t) = -1 + \alpha k \cos(kt), \quad \alpha, k > 0. \quad (21)$$

This form of encodes rich dynamical behavior, oscillating between phases of deceleration and acceleration, thereby capturing the cyclic nature of cosmic evolution. Specifically, ( $q > 0$ ) represents decelerating epochs, ( $q = 0$ ) corresponds to the transition point where expansion proceeds uniformly, ( $q = -1$ ) denotes an exponential de Sitter–like expansion, and ( $q < -1$ ) signals a super-exponential or phantom-like regime. The periodic factor ( $k$ ) regulates the frequency of these alternating phases, effectively setting the cosmic “rhythm,” while the product ( $\alpha k$ ) governs the amplitude of oscillations, dictating the depth of deceleration and acceleration. Moreover, when combined with the sign of the Hubble parameter (18), this model not only distinguishes between accelerated and decelerated states but also differentiates between expansion ( $\sin(kt) > 0$ ) and contraction ( $\sin(kt) < 0$ ), with turning points at ( $\sin(kt) = 0$ ) signifying bounces or recollapses. Thus, the universe undergoes a recurring sequence: beginning with deceleration ( $q = \alpha k - 1$ ,  $\alpha k > 1$ ), smoothly transitioning into accelerated expansion, reaching a super-exponential growth phase, and ultimately returning to deceleration. This cyclical pattern then repeats, offering a unified framework to describe oscillatory cosmologies, bounce dynamics, and the possibility of an eternally recurring universe within the Brans–Dicke framework.

The behavior of the DP, Hubble parameter, and scale factor is depicted in Figures 1, 2, and 3, respectively. Figure 1 clearly demonstrates the oscillatory character of the DP, where the universe alternates between decelerating and accelerating

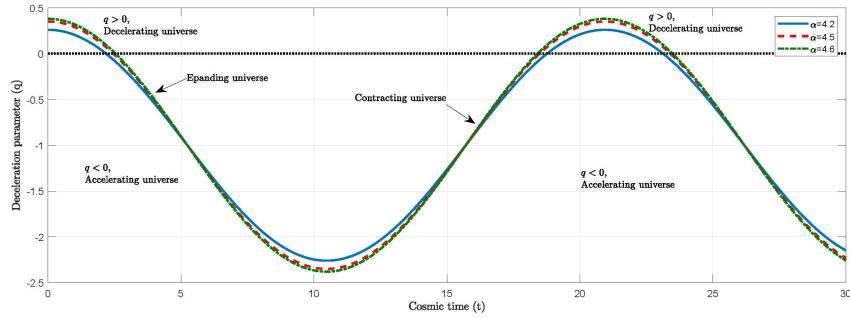


Figure 1. Evolution of the DP  $q(t)$ , showing alternating phases of acceleration and deceleration in each cosmic cycle for  $k = 0.3$ .

phases during expansion, followed by a transition into contraction, and then repeating the same sequence in subsequent cycles. In Figure 2, the Hubble parameter exhibits a similar cyclic pattern, remaining positive during expansion and negative during contraction, thereby characterizing the rhythmic alternation of cosmic growth and collapse. Figure 3 illustrates the corresponding evolution of the scale factor: beginning from a negligible value, it increases during expansion, reaches a turning point, and then decreases during contraction, again resetting for the next cycle. Collectively, these figures provide a consistent and coherent picture of a universe governed by periodic dynamics, undergoing eternal sequences of expansion and contraction in alignment with the proposed model.

The power-law relationship between the scale factor  $a$  and the scalar field  $\phi$ , implies that the scalar field's behavior is intimately tied to the scale factor, with a constant exponent governing this connection. This insight holds key implica-

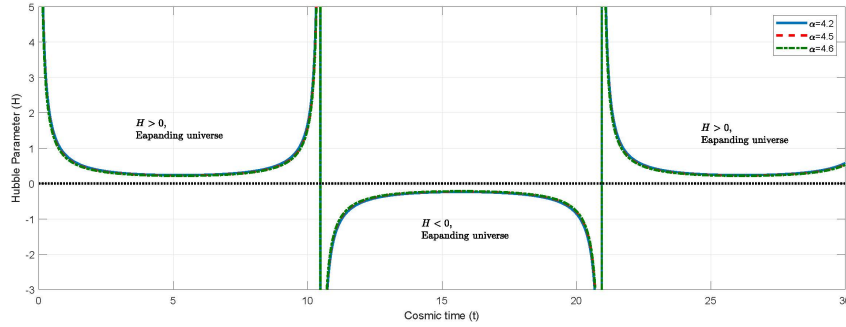


Figure 2. Hubble parameter  $H(t)$  versus cosmic time, oscillating between expansion ( $H > 0$ ) and contraction ( $H < 0$ ) for  $k = 0.3$ .

## 8 Exploring Cyclic Expansion and Contraction in Brans-Dicke Theory ...

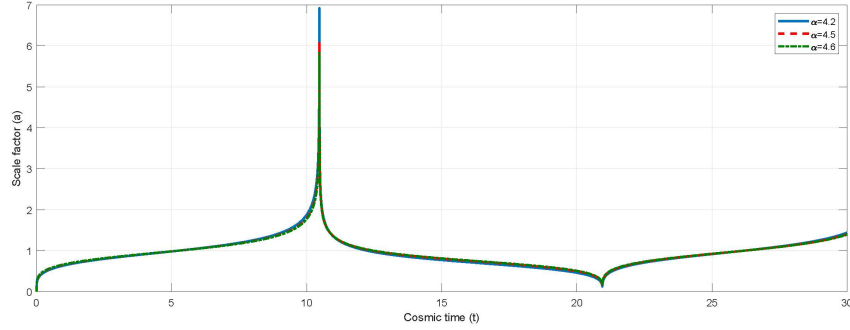


Figure 3. Scale factor  $a(t)$  depicting cyclic growth during expansion and decay during contraction for  $k = 0.3$ .

tions for our understanding of cosmic dynamics. Hence the relation is defined as

$$\phi = \phi_0 a(t)^m, \quad (22)$$

therefore, based on equation (20), the aforementioned equation (22) is transformed as

$$\phi = \phi_0 \left[ \tan \left( \frac{kt}{2} \right) \right]^{\frac{m}{\alpha}}. \quad (23)$$

From equations (6)-(8), we obtain

$$\frac{\ddot{R}_2}{R_2} - \frac{\ddot{R}_3}{R_3} + \frac{\dot{R}_3}{R_3} \left( \frac{\dot{R}_2}{R_2} - \frac{\dot{R}_1}{R_1} \right) + \frac{\dot{\phi}}{\phi} \left( \frac{\dot{R}_2}{R_2} - \frac{\dot{R}_1}{R_1} \right) = 0, \quad (24)$$

$$\frac{\ddot{R}_3}{R_3} - \frac{\ddot{R}_2}{R_2} + \frac{\dot{R}_1}{R_1} \left( \frac{\dot{R}_3}{R_3} - \frac{\dot{R}_2}{R_2} \right) + \frac{\dot{\phi}}{\phi} \left( \frac{\dot{R}_3}{R_3} - \frac{\dot{R}_2}{R_2} \right) = 0, \quad (25)$$

$$\frac{\ddot{R}_3}{R_3} - \frac{\ddot{R}_1}{R_1} + \frac{\dot{R}_2}{R_2} \left( \frac{\dot{R}_3}{R_3} - \frac{\dot{R}_1}{R_1} \right) + \frac{\dot{\phi}}{\phi} \left( \frac{\dot{R}_3}{R_3} - \frac{\dot{R}_1}{R_1} \right) = 0, \quad (26)$$

Solving (24)-(26), we obtain

$$\frac{\dot{R}_1}{R_1} - \frac{\dot{R}_2}{R_2} = \frac{c_1}{R_1 R_2 R_3 \phi}, \quad (27)$$

$$\frac{\dot{R}_2}{R_2} - \frac{\dot{R}_3}{R_3} = \frac{c_2}{R_1 R_2 R_3 \phi}, \quad (28)$$

$$\frac{\dot{R}_3}{R_3} - \frac{\dot{R}_1}{R_1} = \frac{c_3}{R_1 R_2 R_3 \phi}, \quad (29)$$

where  $c_1, c_2$ , and  $c_3$  are integration constants. Equations (27)-(29) further reduces to

$$\frac{R_1}{R_2} = d_1 \exp \left( c_1 \int \frac{dt}{R_1 R_2 R_3 \phi} \right), \quad (30)$$

$$\frac{R_2}{R_3} = d_2 \exp \left( c_2 \int \frac{dt}{R_1 R_2 R_3 \phi} \right), \quad (31)$$

$$\frac{R_3}{R_1} = d_3 \exp \left( c_3 \int \frac{dt}{R_1 R_2 R_3 \phi} \right), \quad (32)$$

where  $d_1, d_2$ , and  $d_3$  are integration constants. Using equations (30)–(32), we can write the directional scalar factors  $R_1, R_2$ , and  $R_3$  explicitly as

$$R_1 = D_1 a \exp \left( C_1 \phi_0^{-1} \int a^{-(m+3)} dt \right), \quad (33)$$

$$R_2 = D_2 a \exp \left( C_2 \phi_0^{-1} \int a^{-(m+3)} dt \right), \quad (34)$$

and

$$R_3 = D_3 a \exp \left( C_3 \phi_0^{-1} \int a^{-(m+3)} dt \right), \quad (35)$$

where  $D_1 = (d_1 d_3^{-1})^{1/3}$ ,  $D_2 = (d_1^{-2} d_3^{-1})^{1/3}$ ,  $D_3 = (d_1 d_3^2)^{1/3}$ ,  $C_1 = (c_1 - c_3)/3$ ,  $C_2 = -(2c_1 + c_3)/3$ , and  $C_3 = (c_1 + 2c_3)/3$ . Which satisfies the relations  $D_1 D_2 D_3 = 1$  and  $C_1 + C_2 + C_3 = 0$ . After simplifying equations (33)–(35), we get

$$R_1 = D_1 \left[ \tan \left( \frac{kt}{2} \right) \right]^{\frac{1}{\alpha}} \exp (C_1 \phi_0^{-1} Q(t)), \quad (36)$$

$$R_2 = D_2 \left[ \tan \left( \frac{kt}{2} \right) \right]^{\frac{1}{\alpha}} \exp (C_2 \phi_0^{-1} Q(t)), \quad (37)$$

and

$$R_3 = D_3 \left[ \tan \left( \frac{kt}{2} \right) \right]^{\frac{1}{\alpha}} \exp (C_3 \phi_0^{-1} Q(t)), \quad (38)$$

where

$$\int a^{-(m+3)} dt = Q(t) = \left( \frac{2^{\frac{3-7\alpha+m}{\alpha}} (kt)^{-\frac{m+3}{\alpha}}}{2835} \right) \left[ \frac{362880\alpha t}{\alpha - (m+3)} - \frac{30240k^2(m+3)t^3}{3\alpha - (m+3)} - \frac{252k^4 \{7\alpha - 5(m+3)\} (m+3)t^5}{\alpha \{5\alpha - (m+3)\}} + \mathcal{O}(t^6) \right].$$

## 10 Exploring Cyclic Expansion and Contraction in Brans-Dicke Theory ...

Therefore the directional Hubble parameters  $H_i$ ,  $i = 1, 2, 3$  takes the form

$$H_1 = \frac{1}{\alpha \sin(kt)} + C_1 \left[ \tan \left( \frac{kt}{2} \right) \right]^{\frac{-m+3}{\alpha}}, \quad (39)$$

$$H_2 = \frac{1}{\alpha \sin(kt)} + C_2 \left[ \tan \left( \frac{kt}{2} \right) \right]^{\frac{-m+3}{\alpha}}, \quad (40)$$

$$H_3 = \frac{1}{\alpha \sin(kt)} + C_3 \left[ \tan \left( \frac{kt}{2} \right) \right]^{\frac{-m+3}{\alpha}}. \quad (41)$$

Thus, the metric (1) can be written as

$$ds^2 = dt^2 - \left[ D_1^2 \exp(2C_1 Q(t)) dx^2 + D_2^2 \exp(2C_2 Q(t)) dy^2 + D_3^2 \exp(2C_3 Q(t)) dz^2 \right] \left\{ \tan \left( \frac{kt}{2} \right) \right\}^{\frac{2}{\alpha}}. \quad (42)$$

Now, we feel the necessity to discuss the physical and geometric properties of the universe within the framework of the proposed study.

### 4 Fundamental Properties and Solutions of the Model

As we know, understanding the physical and geometric properties is crucial, as they provide a concrete comprehension of the universe. Additionally, we will interpret the mathematical results in a meaningful manner. Therefore, to investigate the physical characteristics of the model defined in (42), we shall determine several crucial parameters in equations (12)–(15) that play a significant role in the analysis of cosmological models. Hence, we have determined them as follows:

$$V(t) = \left[ \tan \left( \frac{kt}{2} \right) \right]^{\frac{3}{\alpha}}, \quad (43)$$

$$\theta(t) = \frac{3}{\alpha \sin(kt)}, \quad (44)$$

$$\sigma^2 = A \left[ \tan \left( \frac{kt}{2} \right) \right]^{\frac{-2(m+3)}{\alpha}}, \quad (45)$$

and

$$A_m = \frac{2A}{3} \alpha \sin(kt) \left[ \tan \left( \frac{kt}{2} \right) \right]^{\frac{-2(m+3)}{\alpha}}, \quad (46)$$

where the value of constant  $A$  is  $\frac{1}{2}(C_1^2 + C_2^2 + C_3^2)$ .

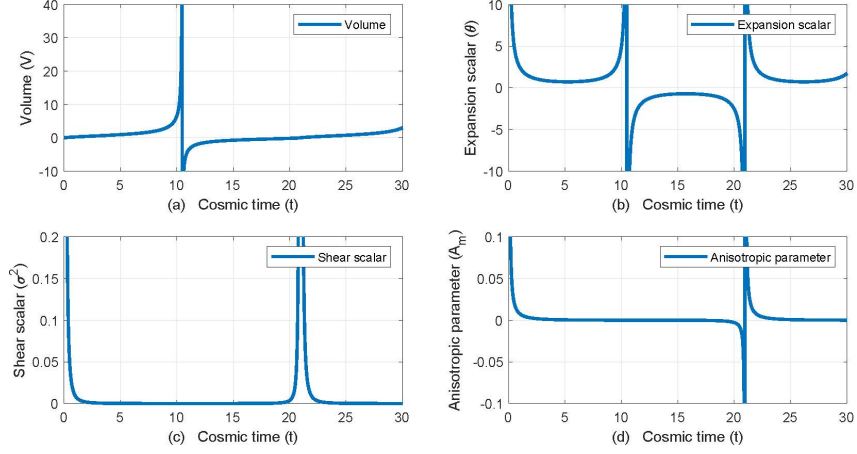


Figure 4. Evolution of kinematic parameters with cosmic time: (a) spatial volume  $V(t)$ , (b) expansion scalar  $\theta(t)$ , (c) shear scalar  $\sigma^2(t)$ , and (d) anisotropy parameter  $A_m(t)$ , illustrating the cyclic expansion and contraction of the universe in successive cosmic cycles for  $\alpha = 4.2$ ,  $k = 0.3$ , and  $c_1 = c_2 = c_3 = 0.1$ .

Figure 4 illustrates the evolution of various kinematic parameters with respect to cosmic time. Subplot (a) depicts the behavior of the spatial volume  $V$ , (b) shows the expansion scalar  $\theta$ , (c) presents the shear scalar  $\sigma^2$ , and (d) displays the anisotropy parameter  $A_m$ .

In subplot (a), the spatial volume begins from zero at  $t = 0$ , marking the initial singular state of the Universe. As time progresses,  $V$  increases, indicating the expanding phase. Subsequently, the volume decreases and becomes negative, reflecting a contracting epoch. Afterward, it re-enters the positive domain, corresponding to a re-expanding phase, thereby confirming the cyclic nature of the Universe. In subplot (b), the expansion scalar  $\theta$  exhibits a trend similar to that of the Hubble parameter. Positive values of  $\theta$  correspond to expanding phases, while negative values indicate contracting phases, again supporting the oscillatory dynamics of the model. Subplot (c) highlights the behavior of the shear scalar  $\sigma^2$ . At  $t = 0$ ,  $\sigma^2$  assumes a very high value, signifying strong anisotropy in the early Universe. As time increases during the expanding phase,  $\sigma^2$  decreases and tends toward zero, indicating isotropization at late times. In the contracting phase, however,  $\sigma^2$  grows again and diverges toward infinity, repeating the same pattern across successive cycles. Finally, subplot (d) shows the anisotropy parameter  $A_m$ , which is initially large at  $t = 0$ . As time evolves during expansion,  $A_m$  decreases and approaches zero, reflecting the trend toward isotropy. In the contracting epoch,  $A_m$  enters the negative region and diverges toward  $-\infty$ , marking the termination of the cycle, after which the same oscillatory behavior recurs.

## 12 Exploring Cyclic Expansion and Contraction in Brans-Dicke Theory ...

Now using equations (5)–(9) and (36)–(38), we derive the expressions for  $\Lambda$ ,  $\rho$ , and  $p$  as

$$\begin{aligned} \Lambda(t) = & \left\{ -\frac{\omega}{2}m^2 + (\alpha - 3)\omega m - 3(\alpha - 2) \right\} H^2 \\ & + (3 - m\omega) \frac{k^2}{2\alpha} \sec^2 \left( \frac{kt}{2} \right) + (C_1^2 - C_2 C_3) \left[ \tan \left( \frac{kt}{2} \right) \right]^{\frac{-2(m+3)}{\alpha}}, \end{aligned} \quad (47)$$

$$\begin{aligned} \rho(t) = & \frac{\phi_0}{8\pi} \left[ \{ (2\omega + 3)m + (m\omega - 3)(1 - \alpha) \} H^2 \right. \\ & + \frac{1}{2\alpha} \left\{ k^2(m\omega - 3) \sec^2 \left( \frac{kt}{2} \right) \right\} \\ & \left. - 2(C_1^2 - C_2 C_3) \left\{ \tan \frac{kt}{2} \right\}^{\frac{-2(m+3)}{\alpha}} \right] \left\{ \left[ \tan \frac{kt}{2} \right]^{\frac{m}{\alpha}} \right\} \end{aligned} \quad (48)$$

and

$$\begin{aligned} p(t) = & -\frac{\phi_0}{8\pi} \left[ \{ (2\omega + 1)m + m(\omega + 1)(m - \alpha + 1) + \alpha - 3 \} H^2 \right. \\ & + \frac{1}{2\alpha} \left\{ k^2(m\omega + m - 1) \sec^2 \left( \frac{kt}{2} \right) \right\} \\ & \left. - C_1^2 \left\{ \tan \frac{kt}{2} \right\}^{\frac{-2(m+3)}{\alpha}} \right] \left\{ \tan \frac{kt}{2} \right\}^{\frac{m}{\alpha}}. \end{aligned} \quad (49)$$

The EoS parameter in cosmology is a crucial factor that characterizes the relationship between pressure and energy density in the universe's components. It plays a central role in determining the past, present, and future dynamics of the cosmos, especially in elucidating the nature of DE and the fate of the universe. The EoS parameter ( $\xi$ ) is defined as the ratio of the pressure to the energy density i.e.,  $\xi = p/\rho$ . We may express the EoS parameter  $\xi$  as under:

$$\begin{aligned} \xi(t) = & -\frac{\phi_0}{8\pi\rho} \left[ \{ (2\omega + 1)m + m(\omega + 1)(m - \alpha + 1) + \alpha - 3 \} H^2 \right. \\ & + \frac{1}{2\alpha} \left\{ k^2(m\omega + m - 1) \sec^2 \left( \frac{kt}{2} \right) \right\} \\ & \left. - C_1^2 \left[ \tan \frac{kt}{2} \right]^{\frac{-2(m+3)}{\alpha}} \right] \left( \tan \frac{kt}{2} \right)^{\frac{m}{\alpha}}. \end{aligned} \quad (50)$$

The evolution of the cosmological constant  $\Lambda$  and energy density  $\rho$  is depicted in Figures 5 and 6, respectively. Both quantities follow a closely similar pattern across cosmic cycles. At  $t = 0$ , corresponding to the bounce, they begin

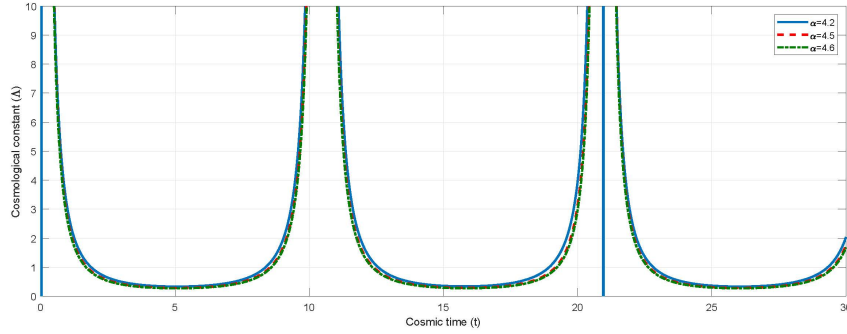


Figure 5. Evolution of the cosmological constant  $\Lambda(t)$ , starting from very high values at the bounce, decreasing during expansion, and diverging again at turnaround, repeating cyclically across cosmic phases for  $m = 2$ ,  $\omega = 1.6$ ,  $k = 0.3$ , and  $c_i = 0.1$ ;  $c_i = 0.1$ ;  $i = 1, 2, 3$ .

with extremely high positive values, signifying the dominance of vacuum and matter-energy at the onset of expansion. As time increases, both  $\Lambda$  and  $\rho$  decrease monotonically, approaching near-zero values at intermediate stages of expansion, indicating a dilution of energy density and weakening of the cosmological constant. Eventually, they rise again towards infinity as the universe approaches the turnaround point, thereby initiating the contraction phase. This cyclical trend continues identically in subsequent cosmic cycles, reinforcing the oscillatory nature of the model.

A similar behavior is observed for the pressure  $p$ , shown in Figure 7, but with an opposite sign. At the bounce ( $t = 0$ ), the pressure takes a very large negative

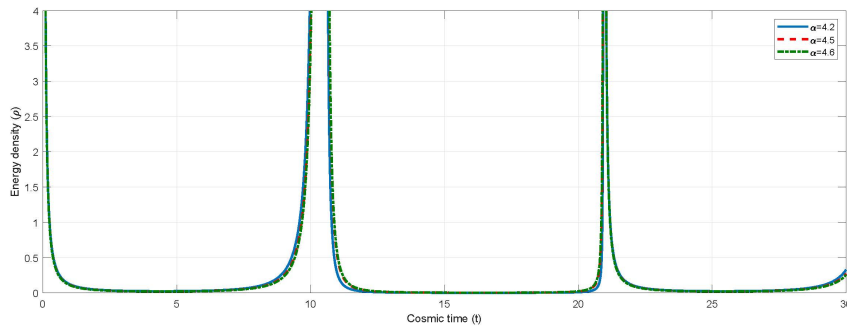


Figure 6. Evolution of the energy density  $\rho(t)$ , exhibiting the same cyclic trend as  $\Lambda$ : high at the bounce, diluted during expansion, and rising again towards infinity at contraction for  $m = 2$ ,  $\omega = 1.6$ ,  $k = 0.3$ ,  $\phi_0 = 1$ , and  $c_i = 0.1$ ;  $i = 1, 2, 3$ .

#### 14 Exploring Cyclic Expansion and Contraction in Brans-Dicke Theory ...

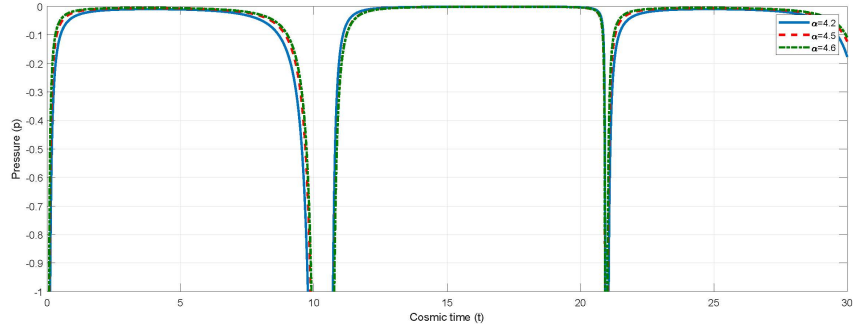


Figure 7. Evolution of pressure  $p(t)$ , beginning with large negative values at the bounce, rising towards zero in mid-expansion, and falling back to negative infinity near turnaround, consistently repeating in each cycle for  $m = 2, \omega = 1.6, k = 0.3 \phi_0 = 1$ , and  $c_i = 0.1; i = 1, 2, 3$ .

value, which drives the rapid expansion phase. With increasing time,  $p$  rises towards zero, indicating a transient balance between expansion and contraction forces, and subsequently falls again towards negative infinity as the universe approaches the end of its expansion. During contraction, the same sequence repeats, ensuring consistency with the cyclic dynamics of the universe.

In Figure 8, the EoS parameter  $\xi$  exhibits an oscillatory behavior with cosmic time, maintaining values strictly in the negative domain. This indicates that the fluid content of the universe consistently behaves like DE. During the expansion phase,  $\xi$  initially decreases towards more negative values, enhancing the repulsive effect responsible for cosmic acceleration. As the universe evolves further,

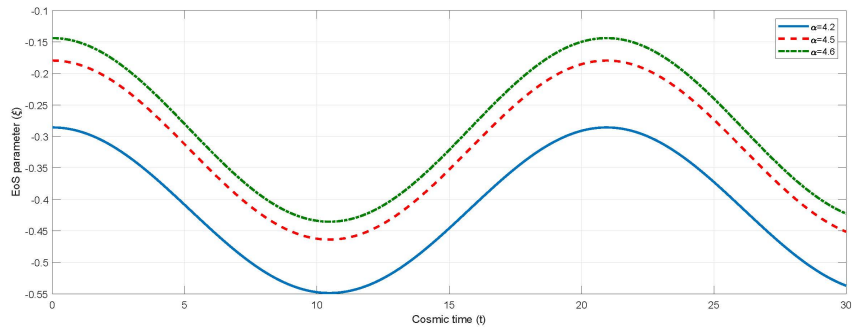


Figure 8. Pictorial illustration of EoS parameter  $\xi(t)$  with time  $t$  for  $m = 2, \omega = 1.6, k = 0.3 \phi_0 = 1$ , and  $c_i = 0.1; i = 1, 2, 3$ .

$\xi$  rises toward less negative values, reducing the dominance of DE and preparing for a transition into the contraction phase. A similar trend repeats in the contracting phase, showing the cyclic nature of the model.

The overall evolution suggests that the universe alternates between stronger and weaker DE effects within each cycle, while never entering into the phantom regime ( $\xi < -1$ ). This ensures that the dynamics remain within a quintessence-like domain, consistent with an oscillatory and nonsingular cosmology.

#### 4.1 Energy conditions

Energy conditions (EC) are important criteria in cosmology used to characterize the physical properties of matter and energy in the universe through their gravitational effects [34, 35]. These conditions—namely the Weak Energy Condition (WEC), Null Energy Condition (NEC), Dominant Energy Condition (DEC), and Strong Energy Condition (SEC)—impose constraints on the EMT within Einstein’s field equations. They serve to ensure that physically reasonable forms of matter and energy do not violate fundamental principles such as positivity of energy density or causal propagation of energy. These conditions play a crucial role in analyzing the expansion, stability, and ultimate fate of the universe.

They are mathematically expressed as:

$$\begin{aligned} \text{WEC: } & \rho \geq 0, \quad \rho + p \geq 0, \\ \text{NEC: } & \rho + p \geq 0, \\ \text{DEC: } & \rho \geq 0, \quad \rho \pm p \geq 0, \\ \text{SEC: } & \rho + p \geq 0, \quad \rho + 3p \geq 0. \end{aligned}$$

Figure 9 illustrates the evolution of the EC across cyclic phases of the universe. At the initial epoch  $t = 0$ , all conditions begin with highly positive values, con-

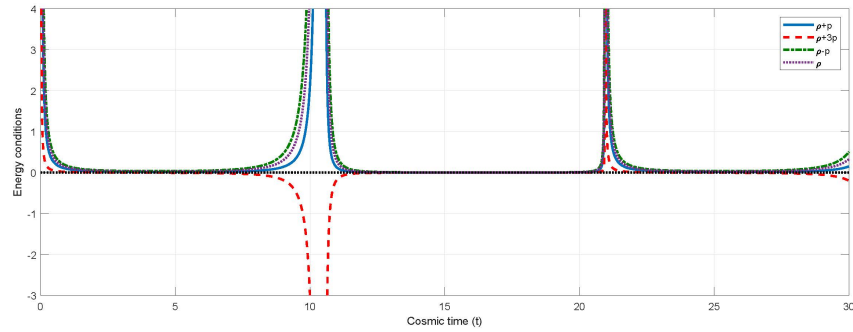


Figure 9. Evolution of the EC across cosmic cycles, highlighting their validity and the SEC violation during accelerated phases for  $m = 2$ ,  $\omega = 0.5$ ,  $k = 0.1$ ,  $\phi_0 = 1$ ,  $c_i = 0.1$  and  $d_i = -20$ ;  $i = 1, 2, 3$ .

sistent with a dense and energetic early state. As time progresses through the expansion phase, the NEC:  $(\rho + p \geq 0)$ , WEC:  $\rho \geq 0, \rho + p \geq 0$ , and DEC:  $(\rho \geq 0, \rho \pm p \geq 0)$  remain satisfied at all times. Their persistence ensures that the matter content maintains physically reasonable energy density, causal propagation of energy, and stability of the cosmic fluid throughout both expansion and contraction.

In contrast, the SEC exhibits a distinctive behavior. During the expanding phase,  $\rho + 3p$  gradually decreases, crosses into the negative domain, and diverges towards  $(-\infty)$  near the end of expansion. This violation of the SEC signals the dominance of repulsive gravity, associated with DE-like effects responsible for cosmic acceleration. In the contracting phase, the trend reverses:  $(\rho + 3p)$  rises from negative values back into the positive regime, diverging towards  $(+\infty)$  as the cycle closes. This indicates the restoration of attractive gravity, which governs the contraction and prepares the universe for a subsequent bounce.

Thus, the NEC, WEC, and DEC consistently validate physically acceptable matter-energy content across cycles, while the cyclic violation and restoration of the SEC provide the dynamical mechanism for alternating phases of expansion and contraction. This interplay elegantly underpins the oscillatory nature of the universe within the present model.

## 5 Cosmographic Analysis

### 5.1 Jerk, snap & lerk parameter

In this section, we adopt a cosmographic approach to explore the evolution of the universe. Cosmographic parameters go beyond the fundamental Hubble constant, offering higher-order insights into cosmic expansion dynamics. These parameters, including jerk, snap, and lerk, are derived from the Taylor expansion of the universe's scale factor ( $a$ ) with respect to cosmic time ( $t$ ). The jerk parameter, denoted as  $j$  represents the third derivative of the scale factor  $a$  with respect to cosmic time  $t$ . It provides information about the rate of change in the cosmic acceleration. In other words, it describes whether the universe's expansion is accelerating at a constant rate or if the rate of acceleration itself is changing. A positive jerk parameter suggests an accelerating acceleration, while a negative value implies a decelerating acceleration. The jerk parameter is valuable in refining our understanding of DE and its evolving influence on the universe. The snap parameter ( $s$ ) is the higher ( $4^{th}$ ) order derivative of  $a$  with respect to  $t$ . It shows whether the rate of acceleration itself is changing over time. Like the jerk parameter,  $s$  helps us understand the nuanced behavior of cosmic acceleration. The lerk parameter ( $l$ ) is the fifth derivative of  $a$  with respect to  $t$ . It provides further insights into changes in the rate of change of acceleration, offering a higher level of detail in characterizing cosmic dynamics.

These parameters enhance our understanding of cosmic evolution, especially in the context of DE. These parameters  $j$ ,  $s$ , and  $l$  [36, 37], being defined by

$$j(t) = \frac{\ddot{a}}{a} \left(\frac{\dot{a}}{a}\right)^{-3}, \quad s(t) = \frac{\ddot{\dot{a}}}{\dot{a}} \left(\frac{\dot{a}}{a}\right)^{-4}, \quad l(t) = \frac{\ddot{\ddot{a}}}{\ddot{a}} \left(\frac{\dot{a}}{a}\right)^{-5}. \quad (51)$$

Initially, we represent these parameters in relation to  $H$  and its derivatives as presented below:

$$j(t) = 1 + \frac{\ddot{H}}{H^3} + 3\frac{\dot{H}}{H^2}, \quad (52)$$

$$s(t) = 1 + \frac{\ddot{\dot{H}}}{H^4} + 4\frac{\ddot{H}}{H^3} + 3\left(\frac{\dot{H}}{H^2}\right)^2 + 6\frac{\dot{H}}{H^2}, \quad (53)$$

$$l(t) = 1 + \frac{\ddot{\ddot{H}}}{H^5} + 5\frac{\ddot{\dot{H}}}{H^4} + 10\frac{\ddot{H}}{H^3} + 15\left(\frac{\dot{H}}{H^2}\right)^2 + 10\frac{\dot{H}\ddot{H}}{H^5} + 10\frac{\dot{H}}{H^2}. \quad (54)$$

Hence we obtained the expressions for  $j$ ,  $s$ , and  $l$  as

$$j(t) = 1 + \alpha^2 k^2 - 3\alpha k \cos(kt) + \alpha^2 k^2 \cos^2(kt), \quad (55)$$

$$s(t) = 1 - \alpha k \{6 + 5\alpha^2 k^2\} \cos(kt) + 3\{\alpha k \cos(kt)\}^2 - \{\alpha k \cos(kt)\}^3, \quad (56)$$

$$l(t) = 1 + 10\alpha^2 k^2 + 5\alpha^4 k^4 - 5\alpha k \{2 + 7\alpha^2 k^2\} \cos(kt) + \alpha^2 k^2 \{25 + 18\alpha^2 k^2\} \cos^2(kt) - 15\{\alpha k \cos(kt)\}^3 + \{\alpha k \cos(kt)\}^4. \quad (57)$$

Graphs for cosmographic parameters (jerk, snap, and lerk) are shown in Figures 10, 11, and 12. Figure 10 depicts the jerk parameter ( $j$ ) graph with a positive trend, indicating accelerating cosmic expansion influenced by growing DE. Subsequent cyclic declines imply periodic deceleration, offering concise insight into complex cosmic dynamics. Figure 11, displaying the snap parameter, reveals a periodic pattern representing alternating cosmic acceleration and deceleration

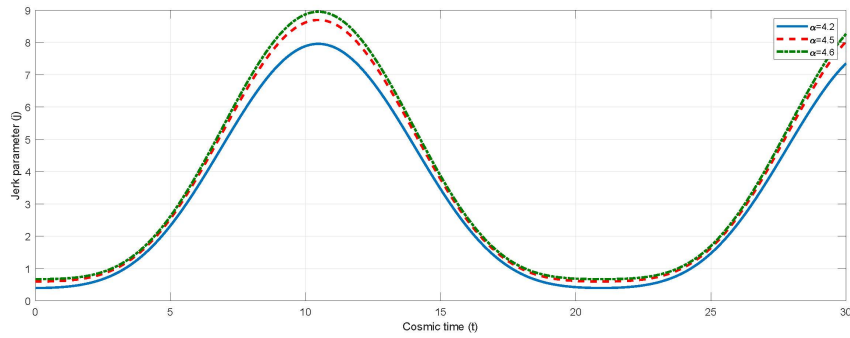


Figure 10. Pictorial illustration of jerk parameter with time  $t$  for  $k = 0.3$ .

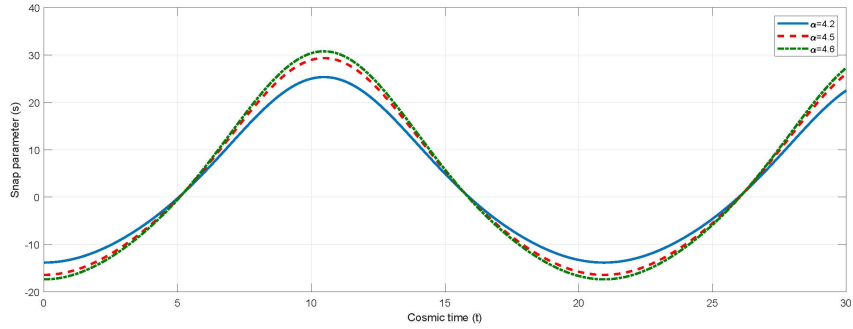


Figure 11. Pictorial illustration of snap parameter with time  $t$  for  $k = 0.3$ .

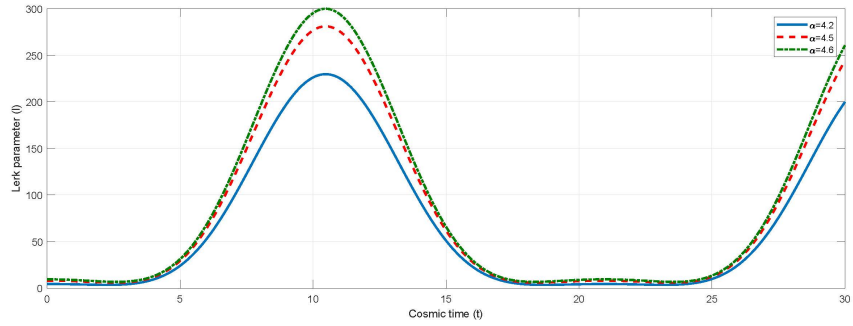


Figure 12. Pictorial illustration of lerk parameter with time  $t$  for  $k = 0.3$ .

phases. The snap parameter ( $s$ ) quantifies the jerk parameter’s rate of change, providing insights into higher-order derivatives of the universe’s scale factor. Its periodic behavior suggests intricate cosmic evolution dynamics, potentially influenced by diverse DE effects or exotic components. Figure 12, showcasing the lerk parameter, exhibits periodicity starting positively, reaching a peak, and cyclically returning. This implies a recurring pattern in cosmic expansion dynamics involving acceleration and deceleration.

## 5.2 Statefinder diagnostic

The statefinder diagnostic is a versatile tool used in cosmology to enhance our understanding of how the universe expands. It goes beyond traditional parameters like the Hubble parameter and DP by introducing higher-order derivatives of the scale factor. By analyzing these statefinder parameters, we can gain deeper insights into cosmic acceleration and the underlying physics driving it.

In the  $\Lambda$ CDM model, these statefinder parameters remain constant over time, reflecting the model's consistent expansion behavior. However, for other models like Chaplygin gas (CG), these parameters change with time, making them distinguishable from  $\Lambda$ CDM. Quintessence models, which involve dynamic DE, exhibit varying statefinder parameter trajectories, indicate insights into the nature of the DE field. On the other hand, standard cold dark matter (SCDM) models have constant statefinder parameters, highlighting their unique expansion dynamics.

The statefinder diagnostic serves as an approach independent of specific models and helps distinguish between models involving DE and standard ones like  $\Lambda$ CDM, standard cold dark matter (SCDM), quintessence, and CG. Sahni et al. (2003) [38] introduced a geometrical pair denoted as  $(r, s)$ , where  $r$  corresponds to the jerk parameter outlined in subsection 5.1. The parameter  $s$  combines  $r$  with the DP  $q$ , and its expression is given as follows:

$$s = \frac{r - 1}{3q - 3/2}. \quad (58)$$

In our analysis, we examine how different DE models evolve by plotting trajectories of this  $(s, r)$  pair on a  $s-r$  plane. In this plane, the fixed point  $(s, r) = (0, 1)$  represents the  $\Lambda$ CDM model. The region of the parameter space where  $s < 0$  and  $r > 1$  defines the CG dark energy model, while the region with  $s > 0$  and  $r < 1$  represents the quintessence DE model.

The value of  $s$  can be calculated using the following equation:

$$s = -\frac{2\{\alpha + k^2 \cot^3(kt) \csc(kt) + 5k^2 \cot(kt) \csc^3(kt)\}}{3\alpha\{-3 + 2\alpha k \cos(kt)\}}. \quad (59)$$

Figure 13 presents the evolutionary trajectory of the statefinder pair  $(s, r)$ , which serves as a powerful diagnostic tool to distinguish DE models. The trajectory begins in the CG domain ( $s < 0, r > 1$ ), a region typically associated with exotic fluids that can mimic both matter and DE behavior at different epochs. As the universe evolves, the trajectory passes through the fixed point ( $s = 0, r = 1$ ), which characterizes the standard  $\Lambda$ CDM cosmology. This crossing indicates that the model reproduces the concordance scenario at a specific stage of evolution, thereby aligning with the current cosmological paradigm.

Subsequently, the path enters the quintessence region ( $s > 0, r < 1$ ), reflecting a phase where DE behaves dynamically with an EoS ( $\xi > -1$ ). This transition highlights the model's capability to unify different cosmic regimes within a single framework: mimicking a CG at early stages, reproducing  $\Lambda$ CDM as an intermediate attractor, and finally evolving towards quintessence-like behavior. Such an evolutionary trajectory underscores the richness of the present model, as it not only connects with standard cosmology but also extends beyond it, offering insights into possible dynamical DE scenarios.

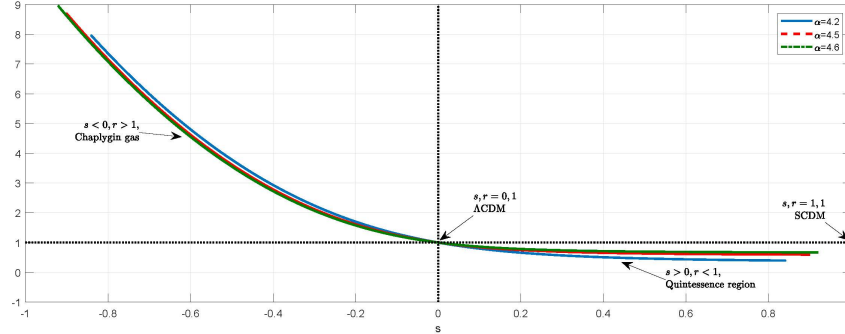


Figure 13. Statefinder trajectory  $(s, r)$  evolving from the CG regime through the  $\Lambda$ CDM point into the quintessence region.

## 6 Concluding remark

In this work, we have investigated the cyclic evolution of the Universe within the framework of BDT by employing a PVDP together with a power-law relation between the scalar field and the scale factor. The solutions obtained for the BI spacetime reveal a Universe that undergoes successive phases of expansion and contraction, thereby exhibiting a consistent bouncing or cyclic behavior.

The kinematic quantities, including the Hubble parameter, expansion scalar, shear scalar, and anisotropy parameter, confirm the oscillatory dynamics and demonstrate a gradual transition from anisotropy to near isotropy over successive cycles. The evolution of energy density, pressure, and cosmological constant shows periodic patterns in accordance with the expansion and contraction epochs, while the EoS parameter oscillates across quintessence and phantom like regimes, further reinforcing the cyclic scenario.

Energy condition analysis indicates that while the Weak, Null, and Dominant EC remain satisfied throughout, the SEC is violated during accelerated epochs. This violation is consistent with the requirements for achieving cosmic acceleration and supports the feasibility of a cyclic Universe. Complementing this, higher-order cosmographic parameters such as jerk, snap, and lerk have been examined, whose oscillatory behavior with cosmic time provides further evidence for alternating phases of acceleration and deceleration, capturing the fine details of cyclic cosmic evolution.

Finally, the statefinder diagnostic  $(s, r)$  shows a trajectory that originates in the CG regime, passes through the stationary point of  $\Lambda$ CDM, and eventually enters the quintessence domain. This evolutionary track highlights the ability of the model to interpolate between different DE scenarios and demonstrates its potential to serve as a viable alternative to standard singular cosmologies.

Overall, the proposed framework encapsulates the recurring birth, evolution, turnaround, and rebirth of the Universe in an oscillatory manner. This cyclic Brans–Dicke model not only aligns with the broader expectations of nonsingular cosmologies but also opens a promising pathway to explore the interplay between scalar–tensor gravity, cosmography, and cyclic Universe paradigms.

### Acknowledgements

The authors express their sincere gratitude to the Mathematics Department of SLIET Longowal for providing the necessary facilities to complete their research.

### References

- [1] S. Perlmutter, et al. (1998) Discovery of a supernova explosion at half the age of the Universe. *Nature* **391**(6662) 51-54.
- [2] A.G. Riess, et al. (1998) Observational Evidence from Supernovae for an Accelerating Universe and a Cosmological Constant. *Astron. J.* **116**(3) 1009.
- [3] S. Perlmutter, et al. (1999) Measurements of  $\Omega$  and  $\Lambda$  from 42 high-redshift supernovae. *Astron. J.* **517**(2) 565.
- [4] D.N. Spergel, et al. (2003) First-year Wilkinson Microwave Anisotropy Probe (WMAP)\* observations: determination of cosmological parameters. *Astrophys. J. Suppl. Ser.* **148**(1) 175.
- [5] A.E. Lange, et al. (2001) Cosmological parameters from the first results of Boomerang. *Phys. Rev. D* **63**(4) 042001.
- [6] M.S. Berman, F. de Mello Gomide (1988) Cosmological models with constant deceleration parameter. *Gen. Relativ. Gravit.* **20**(2) 191-198.
- [7] R.K. Mishra, N. Jain (2024) Cosmic Dynamics Beyond Einstein Theory: Mathematical Analysis with  $f(R, T)$  Gravity. *Int. J. Theor. Phys.* **63**(1) 29.
- [8] D.R.K. Reddy, R.N. Venkateswara (2001) Some cosmological models in scalar-tensor theory of gravitation. *Astrophys. Space Sci.* **277** 461-472.
- [9] M.F. Shamir, A.A. Bhatti (2020) Anisotropic dark energy Bianchi type III cosmological models in the Brans–Dicke theory of gravity. *Can. J. Phys.* **90**(2) 193-198.
- [10] R.K. Mishra, R. Sharma (2025) Comparative study of linear & non-linear  $f(T)$  gravity models in Bianchi type-III space-time. *Astrophys. Space Sci.* **370** 2.
- [11] R.K. Mishra, N. Jain (2024) Stability analysis in cosmological models using perturbative methods in  $f(R, T)$  theory. *Rom. J. Phys.* **69** 113.
- [12] S.R. Hadole, A.S. Nimkar (2024) A Comparative Study of Cosmological Models in Barber Self Creation Theory of Gravitation. *Bulg. J. Phys.* **51**(2) 117-129.
- [13] R.K. Mishra, R. Sharma (2024) Certain investigations on Bianchi-III cosmological model with FLVDP in  $f(R, T)$  theory. *Bulg. J. Phys.* **51**(3) 218-241.
- [14] R.K. Mishra, R. Sharma (2025) Decoding the universe: A comparative study of cosmographic parameters within  $f(R, T)$  gravity. *Mod. Phys. Lett. A* **40**(24) 2550086.
- [15] J.S. Wath, A.S. Nimkar (2023) Cosmological Parameters and Stability of Bianchi Type-VIII in Sáez-Ballester Theory of Gravitation. *Bulg. J. Phys.* **50** 3 255-264.

- [16] N. Jain, R.K. Mishra (2025) Numerical and statistical insights into  $f(R, T)$  cosmology: GRP, RK4, and MLE approaches. *Astrophys. Space Sci.* **370**(8) 89.
- [17] R. Sharma, A. Chand, R.K. Mishra (2023) Cosmological model in  $f(R, T)$  theory with time-varying FLVDP. *J. Phys. Conf. Ser.* **2663**(1) 012055.
- [18] S.S. Nerkar, S.B. Deshmukh (2025) Dynamics of Bianchi Type-III Universe in  $f(T)$  Gravity. *Bulg. J. Phys.* **52**(3) 265-276.
- [19] C. Brans, R.H. Dicke (1961) Mach's principle and a relativistic theory of gravitation. *Phys. Rev.* **124**(3) 925.
- [20] R. Sharma, R.K. Mishra (2025) Unrevealing Cosmic Geometry: Bianchi-III Cosmology in BDT with FLVDP. *Bulg. J. Phys.* **52**(3) 237-254.
- [21] S. K. Tripathy, S. K. Pradhan, Z. Naik, D. Behera, B. Mishra (2020) Unified dark fluid and cosmic transit models in Brans–Dicke theory. *Phys. Dark Universe* **30** 100722.
- [22] S.K. Tripathy, S.K. Pradhan, B. Barik, Z. Naik, B. Mishra (2023) Evolution of Generalized Brans–Dicke Parameter within a Superbounce Scenario. *Symmetry* **15**(4) 790.
- [23] R.K. Mishra, R. Sharma (2024) Exploring the Bianchi-IX universe within Brans–Dicke theory and a deceleration parameter. *Mod. Phys. Lett. A* **39**(35n36) 2450169.
- [24] R.K. Mishra, N. Jain (2025) Beyond four dimensions: An extended study of  $f(R, T)$  theory with multidimensional metric. *Int. J. Geom. Methods Mod. Phys.* **22**(4) 2450310-192.
- [25] G. Kofinas, M. Tsoukalas (2016) On the action of the complete Brans–Dicke theory. *Eur. Phys. J. C* **76**(12) 686.
- [26] R.K. Mishra, R. Sharma (2024) Beyond general relativity: comparative analysis between BDT and  $f(R, T)$  with NLDP. *Eur. Phys. J. Plus* **139**(8) 692.
- [27] M. Shen, L. Zhao (2014) Oscillating quintom model with time periodic varying deceleration parameter. *Chin. Phys. Lett.* **31**(1) 010401.
- [28] P. Sahoo, S. Tripathy, P. Sahoo (2018) A periodic varying deceleration parameter in  $f(R, T)$  gravity. *Mod. Phys. Lett. A* **33**(33) 1850193.
- [29] N. Ahmed, S.Z. Alamri (2019) A cyclic universe with varying cosmological constant in  $f(R, T)$  gravity. *Can. J. Phys.* **97**(10) 1075–1082.
- [30] R.K. Mishra, R. Sharma (2024) Cosmic acceleration & deceleration with  $f(R, T)$  gravity. *Mod. Phys. Lett. A* **39**(11) 2450044.
- [31] Y. Myrzakulov, A.H. Alfedeel, M. Koussour, E. Hassan, S. Muminov, J. Rayimbaev (2025) A stable and singularity-free oscillating universe in  $f(R, L_m)$  gravity. *Indian J. Phys.* **99** 4883–4891.
- [32] M. Novello, S.P. Bergliaffa (2008) Bouncing cosmologies. *Phys. Rep.* **463**(4) 127-213.
- [33] V.B. Johri, K. Desikan (1994) Cosmological models with constant deceleration parameter in Brans-Dicke theory. *Gen. Relativ. Gravit.* **26**(12) 1217-1232.
- [34] M. Visser, C. Barcelo (2000) Energy conditions and their cosmological implications. In *COSMO-99. Proceedings of the Third International Workshop on Particle Physics and the Early Universe, ICTP, Trieste, Italy, 27 September – 2 October 1999*, eds. U. Cotti, R. Jeannerot, G., A. Smirnov, pp. 98-112.

- [35] C. Molina-Paris, M. Visser (1999) Minimal conditions for the creation of a Friedman–Robertson–Walker universe from a “bounce”. *Phys. Lett. B* **455**(1-4) 90-95.
- [36] M. Visser (2004) Jerk, snap and the cosmological equation of state. *Class. Quantum Grav.* **21**(11) 2603.
- [37] M. Visser (2005) Cosmography: Cosmology without the Einstein equations. *Gen. Relativ. Gravit.* **37** 1541-1548.
- [38] V. Sahni, T.D. Saini, A.A. Starobinsky, U. Alam (2003) Statefinder—a new geometrical diagnostic of dark energy. *J. Exp. Theor. Phys.* **77** 201-206.